Dynamics of corticocortical brain functional connectivity relevant to therapeutic response to biologics in inflammatory arthritis

Authors: Nobuya Abe[1], Kodai Sakiyama[1], Yuichiro Fujieda[1]*, Khin K. Tha[2,3], Hisashi Narita[4], Kohei Karino[1], Masatoshi Kanda[1,5], Michihito Kono[1], Masaru Kato[1], Tatsuya Atsumi[1]

Affiliations:

[1]Department of Rheumatology, Endocrinology and Nephrology, Faculty of Medicine and Graduate School of Medicine, Hokkaido University, Sapporo, Japan.

[2]Department of Diagnostic and Interventional Radiology, Hokkaido University Hospital, Sapporo, Japan.

[3]Global Centre for Biomedical Science and Engineering, Faculty of Medicine, Hokkaido University, Sapporo, Japan.

[4]Department of Psychiatry, Faculty of Medicine, Hokkaido University, Sapporo, Japan.

[5]Department of Rheumatology and Clinical Immunology, School of Medicine, Sapporo Medical University, Sapporo, Japan.

***Corresponding author:** Yuichiro Fujieda, M.D., Ph.D.

Department of Rheumatology, Endocrinology and Nephrology, Faculty of Medicine, Hokkaido University, Kita 15, Nishi 7, Kita-ku, Sapporo, 0608648, Japan.

Email: edaichi@med.hokudai.ac.jp;

Telephone number: +81117065915; Fax number: +81117067710

ORCID: 0000-0003-4705-341X

Keywords: resting-state functional magnetic resonance imaging; dynamic functional connectivity; neuroimaging; rheumatoid arthritis; spondyloarthritis; biologics; inflammatory arthritis; disease activity; brain function

Manuscript Types: Full-length

Abstract word counts: 240

Main text word counts: 2997

Number of Figures: 3

ABSTRACT

Objectives: Brain function controls cognition and pain perception. The dynamics of brain function also affects physiopsychological status in individuals with neuropsychiatric diseases or chronic pain, and could be evaluated by functional magnetic resonance imaging (fMRI). The brain functional connectivity is aberrant in inflammatory arthritis (IA) including rheumatoid arthritis and spondyloarthritis. We aimed to evaluate the effects of dynamic functional connectivity on clinical course of IA in the context of therapeutic responsiveness to biologics using resting-state fMRI.

Methods: Resting-state fMRI data from 64 patients with IA consisting of two cohorts were used. Dynamic functional connectivity was derived as a correlation coefficient of the windowed blood oxygen level-dependent signal time series. We determined representative whole-brain functional connectivity patterns by *k*-means++ cluster analysis, and evaluated the association of their occurrence probability and therapeutic outcomes with biologics.

Results: Four distinct clusters of dynamic functional connectivity in IA patients were determined. In the first cohort, occurrence probability of cluster 3 was associated with favorable therapeutic response in disease activity and patients' global assessment. This finding was validated by the second cohort. The whole-brain functional coordination of the cluster 3 indicated significantly increased corticocortical connectivity, and probabilistically decreased after therapy in treatment-effective patients compared to -ineffective patients.

Conclusion: Dynamic functional connectivity, in particular, frequent emergence of corticocortical connections was associated with clinical outcomes in patients with IA. Our study suggested that the coherence of corticocortical interactions is related to top-down modulation of pain and therapeutic satisfaction, and give significant perspective for brain function in IA management.

INTRODUCTION

In autoimmune inflammatory arthritis (IA) such as rheumatoid arthritis (RA) and spondyloarthritis (SpA), disease activity status including patients' global assessment and systemic inflammation levels are affected by brain function, which could regulate perception and peripheral immunity.

Functional magnetic resonance imaging (fMRI) can detect blood oxygen level-dependent (BOLD) signals that reflect functional activity in each brain region, and functional connectivity between brain regions can be calculated using Pearson's correlation (1). In IA, previous fMRI studies demonstrated the clinical utility of assessing functional connectivity between brain regions. For instance, higher levels of inflammation are associated with more positive connectivity among the inferior parietal lobule, medial prefrontal cortex, and multiple brain networks, and these patterns of connections predicted the presence of increased fatigue and pain in RA patients (2, 3). It is reported that a significant positive correlation between default-mode network connectivity to the left insula and a continuous measure of the degree of fibromyalgia in RA exists (4). Interestingly, RA patients with fibromyalgia showed peripheral inflammation through pronociceptive patterns of brain connectivity between insula and anterior cingulate cortex (ACC) (5). In patients with chronic pain, previous researches demonstrated that brain functional connectivity could predict clinical course of the disease in terms of pain chronification and pharmacologic response (6, 7). We have previously demonstrated that functional connectivity between left insular cortex and ACC was associated with therapeutic responsiveness to biologics in patients with IA (8).

The general method for calculating functional connectivity uses the entire BOLD time series derived from a prolonged period of fMRI acquisition to generate a summary correlation, which is termed static functional connectivity. However, brain functional connectivity actually fluctuates over time, indicating that the static methods for functional connections would be too simple to estimate the whole picture of resting-state brain functions in a given patient (9). To overcome

this problem, dynamic functional connectivity matrices were extracted from the acquired fMRI data by the sliding-window approach segmenting the BOLD time series (10).

Although the association of resting-state dynamic functional connectivity with clinical outcomes has been evaluated in the realm of chronic pain like fibromyalgia or osteoarthritis (11, 12), its clinical utility is unknown in patients with IA. Thus, in the current study we investigated the association of resting-state dynamic functional connectivity with longitudinal clinical parameters in IA patients.

PATIENTS and METHODS

Patients

Patients who met 2010 American College of Rheumatology (ACR) RA classification criteria (13), or Assessment of SpondyloArthritis international Society (ASAS) classification criteria for axial and peripheral SpA (14, 15) were selected. Data of patients with RA and SpA from two cohorts, which include 33 patients and 31 patients, respectively, were collected at Hokkaido University Hospital from 2018 to 2019 and 2019 to 2020, respectively (Supplementary Table 1, 2). These patients needed therapeutic intensification by biological disease modifying anti-rheumatic drugs and were clinically evaluated before and three months after initiation of therapy (Supplementary Table 3, 4). Clinical assessments for RA included a simplified disease activity index (SDAI) (16). Twenty-eight joints for tender joint count (TJC) and swollen joint count (SJC) which include shoulders, elbows, knees, wrists, and each finger and thumb (metacarpophalangeal or proximal interphalangeal joints). Patient's global assessment (PGA) and evaluator's global assessment (EGA) are assessed by a visual analogue scale scored from 0 to 10. Clinical assessments for SpA included Ankylosing Spondylitis Disease Activity Score (ASDAS)-C-reactive protein (CRP), which is calculated by the degrees of back pain and peripheral pain/swelling, morning stiffness duration, PGA and serum level of CRP (17). The patients were functionally evaluated by the modified Health Assessment Questionnaire (mHAQ) for patients' functional status in daily living activities (range: 0-3.0) and Fibromyalgia Impact Questionnaire (FIQR) for evaluating the total spectrum of problems related to fibromyalgia. FIQR contains 3 domains regarding (i) function for daily living, (ii) overall impact for accomplishing goals and overwhelmed state, and (iii) symptoms such as pain, fatigue and mental difficulty, graded on a 0–10 numeric scale in each item. Effective response was defined as at least 20% improvement in ACR core set of disease activity measures in RA (18), and ASAS 20 improvement (19). We obtained written-informed consent for the study and publication from all participants. The study protocol was approved by the Institutional Review Board of Hokkaido

University Hospital (reference number: 010-0031, 018-0128 and 018-0222). The present study complied with the Declaration of Helsinki.

Image acquisition

All brain imaging data were acquired on a 3.0 T MRI scanner (Achieva TX, Philips Medical Systems) and a standard 32-channel radio-frequency head coil (Philips Medical Systems, Best, the Netherlands) at Hokkaido University. The IA patients in the second dataset were scanned twice, before and three months after initiation of therapy. T2*-weighted images were acquired with an echo-planar imaging (EPI) sequence for 7 minutes. The parameters used were as follows: repetition time (TR) 3,000 ms, echo time (TE) 30 ms, flip angle 80°, field of view 24 cm × 24 cm, matrix size 64 × 64, slice thickness 3.3 mm, interslice gap 3.3 mm, 48 axial slices, 140 volumes. During the scanning, the patients were instructed to rest calmly with their eyes open, not to sleep, and not to undergo any cognitive task. The structural T1 magnetization-prepared rapid gradient echo (MPRAGE) images of the head were also acquired with the following parameters: TR 7 ms, TE 3 ms, flip angle 8°, field of view 24 cm × 24 cm, matrix size 256 × 256, slice thickness 1.2 mm, interslice gap 1.2 mm, 170 sagittal slices.

Data preprocessing

Preprocessing was performed using Statistical Parametric Mapping 12 software (SPM12; Wellcome Department of Cognitive Neurology, London, UK) and the CONN toolbox (www.nitrc.org/projects/conn) implemented in MATLAB (Mathworks, Natick, MA, USA). In the preprocessing pipeline, motion correction, realignment, slice-timing correction, outlier identification, coregistration to structural scan, segmentation, normalization to Montreal Neurological Institute (MNI) space, and spatial smoothing (8 mm Gaussian kernel) were performed. Structural scans were skull stripped, and segmented into grey matter, white matter and cerebrospinal fluid masks using the SPM 12 unified segmentation approach. For functional data, the four initial volumes were discarded for the magnetic field's stabilization. Motion

artifact was detected with the artifact detection toolbox (ART toolbox). Outliers' images were added as nuisance regressors within the first-level general liner model (GLM). The noise was estimated and regressed out with CompCor, a component-based noise correction method. The white matter and cerebrospinal fluid masks were used as noise ROIs and regressed. A temporal band-pass filter of 0.008 to 0.09 Hz was applied to the time series for the removal of high-frequency activity associated with cardiac and respiratory activity. Residual BOLD time series were yielded to be extracted. A total of 132 atlas-based regions of interest (ROIs) from FSL Harvard-Oxford Atlas maximum likelihood cortical and subcortical atlas, and AAL atlas for cerebellum were used. For a detailed analysis of insular cortex (IC), we used probabilistic atlases of insular subregion, which included anterior IC consisting of anterior pole, anterior short gyrus, middle short gyrus and posterior short gyrus, and posterior IC consisting of anterior long gyrus and posterior long gyrus (Supplementary Table 3) (20).

Dynamic functional connectivity analysis and clustering algorithm

Dynamic functional connectivity is a correlation coefficient of the windowed time series for characterizing temporal variability in functional connectivity. In the first level analysis, the sliding window approach was employed to estimate the windowed BOLD time series. The time course was segmented into 36-second windows, sliding the onset of each window by 18 seconds for a total of 18 windows (10). Fisher's transformed correlation coefficient was computed in each sliding window between the windowed time course of the ROIs. In the second-level analysis, we initially evaluated recurrent connectivity patterns across IA patients in the dataset of first cohort (n = 33) as previously reported (21). In brief, we first restructured each ROI-to-ROI matrix in one row (*Combination(132,2)* = 8646 dimensions) and window in the other dimension (18 rows). Second, we coupled all the matrices by the time dimension, producing a matrix of 8646 × 18 × 33 (number of patients) elements. Finally, the *k*-means++ cluster analysis algorithm was applied to the yielded matrix using cosine similarity metric. The clustering algorithm was applied 500 times to avoid local minimal value using a random initialization of centroid positions in each

iteration. As a result, we acquired (i) *k* cluster centroids measured by cosine similarity (132 × 132 matrices), and (ii) a cluster label for the pattern corresponding to each matrix of the time window. Representative centroid matrices with functional connectivity values as recurrent patterns were calculated as averages of ROI-to-ROI matrices in each cluster pattern. For the second cohort's dataset, we computed the cosine similarity between each functional connectivity matrix and the cluster centroids determined in the first dataset. Each matrix in the second dataset was then assigned the centroid label that minimized its distance with the centroids. Using the generated clustering, we calculated the occurrence probability of each cluster pattern for each individual. The top 10% ROI-to-ROI correlations within the absolute value of functional connectivity > 0.2 are rendered on the axial anatomical brain view, which were generated by BrainNet Viewer software (22).

Statistical analysis

Analysis of covariance (ANCOVA) adjusting age and sex as confounds, or paired t-test was used to compare the unpaired or paired values of continuous variables, respectively. For multiple comparisons, we used Tukey-Kramer method to derive family-wise-error (FWE)-corrected p-value. Pearson product-moment correlation coefficient was used for a linear correlation. A receiver operating characteristic (ROC) analysis was performed to evaluate the accuracy for therapeutic responsiveness by functional connectivity value with the area under the curve (AUC). A mixed model was used for a repeated measures design with first-order autoregressive model (AR(1)) covariance structure adjusting age, sex and time-windows as fixed effects.

To better understand the identified cluster patterns, differential functional connectivity in each cluster pattern was explored via the ROI-based inferences method. In brief, we defined a different set of connections for each row of the cluster-centroid matrix to classify all connections arising from the same ROI as a new set. We then performed a multivariate parametric GLM for all connections included in each of these new sets, generating an F-statistic for each ROI and a related uncorrected ROI-level p-value. Applying the Benjamini-Hochberg method, false

discovery rate (FDR)-corrected ROI-level p-value was calculated as the expected proportion of false discoveries among all ROIs. In each statistically significant functional connectivity, we extracted the most differential functional connectivity with statistical significance in each cluster pattern by post-hoc Tukey-Kramer multiple comparison tests.

We used JMP Pro 14 (SAS Institute Inc., Cary, NC, USA) or MATLAB (Mathworks, Natick, MA, USA) for all analyses. The analysis results were considered to demonstrate statistical significance when the p-value including FDR- and FWE-corrected values was below 0.05. All statistical tests were two-sided.

RESULTS

Four distinct patterns of dynamic functional connectivity in patients with IA

We first partitioned the dynamic functional observations using the first dataset via *k*-means++ clustering, and the results enabled us to find distinct brain-wide coordination patterns (Figure 1A). The number of clusters *k* was determined through exploratory analyses varying *k* from 3 to 7 (Supplementary Figure 1A). Although a minimal intraclass correlation coefficient was obtained in the five cluster patterns ($k = 5$), the first pattern in cluster 5 was self-correlated with the other patterns from second to fifth (Supplementary Figure 1B). Even when the second to fifth pattern in cluster 5 were used, these modified four cluster patterns showed a lower intraclass correlation coefficient than the original four cluster patterns (Supplementary Figure 1C). Therefore, the number of clusters $k = 4$ (from the second to fifth pattern in the cluster $k = 5$) was adopted (Figure 1B). Among the cluster patterns, 5243 differentially correlated functional connections with statistical significance were detected (Figure 1C). We then applied the second dataset to the above separated clusters for validation.

Dynamic functional connectivity pattern in association with therapeutic response

The occurrence probability analysis of the connectivity patterns in the first dataset demonstrated that emerging pattern of cluster 4 was the least probable (Figure 2A), which was duplicated with the clusters of the second dataset (Figure 2B). In addition, in the first data set, the emergence rate of cluster 3 was higher in IA patients who responded favorably to biologics than those who did not (Figure 2C). In the second dataset, the occurrence of cluster 3 was more probable in the treatment-effective group than the treatment-ineffective group (Figure 2D), consistent with the results obtained from the first data set. The occurrence probability of cluster 3 was significantly associated with therapeutic responsiveness both in the first dataset with AUC 0.7462 (0.5771-0.9152) and in the prospective dataset with AUC 0.7083 (0.5224-0.8943) (Figure 2E, F). Furthermore, the occurrence probability of cluster 3 had a significant positive correlation with

the therapeutic improvement rate of disease activity scoring by SDAI and ASDAS, and PGA (Figure 2G, H).

Dynamic corticocortical connectivity between left insular cortex and anterior cingulate cortex for therapeutic responsiveness

We examined what neurobiological features the cluster patterns represented, and detected that cluster 3 represents higher functional corticocortical correlations including subcortical regions, compared with the other cluster patterns (Figure 3A). On the other hand, the clusters 1, 2, and 4 represent the differential functional correlations in the frontoparietal cortex, cerebellum and subcortex itself, respectively (Supplemental Figure 2A-C). We previously found that static functional connectivity between left anterior insular long gyrus and ACC was related to treatment responsiveness in IA patients (8). Therefore, we evaluated dynamic functional connectivity between ACC and left anterior long IG for treatment efficacy in IA patients. The dynamic functional correlations between these brain regions corresponding to the windows were extracted from the both datasets (Supplementary Figure 2D, E). Results indicated that dynamic functional connectivity values were higher in the treatment effective group than the treatment ineffective group of the both datasets (Figure 3B, C).

Effect on the emergence probability of dynamic functional patterns by biologics

Finally, we analyzed the therapeutic effects on the emergence probability of dynamic functional connectivity clusters using the consolidated dataset (Supplementary Table 6). In the IA patients treated with tumor necrosis factor-α (TNF-α) inhibitors (n = 21), the occurrence probability of cluster pattern 3 was significantly higher in patients who responded favorably to biologic treatment than those who did not (Figure 4A). Also, the occurrence probability of cluster pattern 3 tended to be associated with therapeutic responsiveness in the IA patients treated with non-TNF-α inhibitors (n = 43) (Figure 4B). We analyzed whether therapeutic intervention itself affected the emergence probability of cluster 3 or not, using the fMRI data three months after

biological therapy in the second dataset. It was decreased in the patients with therapeutic effectiveness while it was stable at low level in the patients with therapeutic ineffectiveness (Figure 4C).

DISCUSSION

In this study, we aimed to study the brain's dynamic organization, which determines patterns of functional connectivity associated with therapeutic responsiveness to biologics in IA patients. Results of our study identified that the dynamic patterns of long-standing functional correlations, especially high coherence of corticocortical connectivity, were associated with the improvement of disease activity and PGA by any biological treatments in IA patients. Furthermore, the occurrence probability of corticocortical dynamic pattern was reduced by biological treatments.

The dynamic states of whole-brain functional connectivity assessed by fMRI can demonstrate the flexibility of functional brain networks and capture the patterns of their transient alterations. The whole-brain patterns are widely associated with the physiopsychological status, indicating that distinct dynamic functional connectivity patterns would represent whole-brain functional configurations, which regulate the cognition, perception, and so on. Particularly, our study demonstrated that the occurrence probability of increased corticocortical functional correlations was related to treatment response in patients with IA. Cortical networks have been reported to be associated with pain processing via several mechanisms that represent and modulate pain. The cerebral cortex would regulate pain through interruption of noxious transmission from the spinal cord by activating the descending pain modulatory systems (23). For instance, ACC, the insular cortex, the somatosensory cortices, the ventrolateral orbital cortex and the motor cortex have been proposed to be involved in the modulation of nociceptive processing. A previous report demonstrated decreased resting-state functional connectivity of the sensorimotor cortical network in patients with chronic pain (24). Furthermore, occurrence probability of dynamic functional connectivity among brain cortical regions such as the prefrontal cortex, the posterior cingulate cortex and the angular gyrus, which construct default-mode network was positively associated with pain threshold (25). In previous reports, biological treatments successfully reduced the activity of cortical regions including somatosensory cortex. Treatment with anti-TNF-α antibodies significantly decreased fMRI-assessed BOLD signals in the brain areas of RA

patients within 24 hours (26). Interestingly, responders to TNF-α antibodies showed significantly higher baseline brain activation in somatosensory cortex and association cortex than non-responders (27). Similar response was also observed in Crohn's disease (28). As well as TNF-α, proinflammatory cytokines like IL-6 and IL-17 activate peripheral nociceptive afferents, sending inflammatory signals to the brain (29).

Based on these previous findings, a possible interpretation of our results is that the low coherence of resting-state corticocortical interactions would be associated with the dysfunction of regulating top-down modulation of disability and pain, which may lead to less therapeutic efficacy such as insufficient improvement of disease activity regarding the subjective measure as PGA, although effective anti-rheumatic treatments have been shown to substantially reduce systemic inflammation levels. Proinflammatory cytokines would activate cortices to compensate the top-down controls. Results of the current study implied that anti-cytokine therapies could suppress corticocortical functional connectivity in the IA patients, which may partly account for the favorable responses observed. In other words, intrinsic structural and functional alterations of brain connectivity with the low coherence of resting-state corticocortical associations possibly lead to pain chronification and therapeutic unsatisfaction (30), as seen in the IA patients of our study, who did not satisfactorily respond to biological therapies. Not only systemic inflammation status but also brain functional status would be both important for the management of patients with IA. In IA patients with low cortical activation despite high disease activity, therapeutic approaches from the point of brain cortical function as well as anti-inflammatory treatments may be beneficial.

We acknowledge several limitations of this study. First, this study included a fairly small number of IA patients. Second, this study is of a retrospective nature. However, we were able to duplicate the findings from the first dataset with the second dataset, and we believe that the validated results strengthen the reliability of the findings obtained.

In conclusion, our study demonstrated that the dynamic pattern of functional connectivity was associated with therapeutic responsiveness to biologics in IA patients. Our data suggest that altered top-down regulation observed as resting-state dynamic changes of corticocortical connectivity coherence would affect the clinical course of IA, and fMRI data of the brain as well as systemic inflammatory status may be of value to assess the therapeutic effect of biologics. Our study implies that brain function plays an important role in determining the course of IA and effectiveness of anti-rheumatic therapies.

FUNDING STATEMENTS

No specific funding was received from any bodies in the public, commercial or not-for-profit sectors to carry out the work described in this article.

CONFLICTS OF INTEREST

M.Kono has received research grants from Astellas, GlaxoSmithKline, Kowa Company, Mitsubishi Tanabe, Nippon Shinyaku, Safofi, Taiju Life Social Welfare Foundation, Taisho Pharmaceutical and Terumo Corporation, outside the submitted work; M.Kato has received research grants from AbbVie, Actelion, and GlaxoSmithKline, and speaking fees from Eli Lilly, outside the submitted work; T.A. has received research grants from Alexion, Astellas, AstraZeneca, Chugai Pharmaceutical, Daiichi Sankyo, Mitsubishi Tanabe, Otsuka Pharmaceutical, Pfizer and Takeda Pharmaceutical, and personal fees from AbbVie, Astellas, Boehringer Ingelheim, Bristol-Myers Squibb, Chugai Pharmaceutical, Daiichi Sankyo, Eisai, Eli Lilly, Medical & Biological Laboratories, Mitsubishi Tanabe, Novartis, Ono Pharmaceutical, Pfizer, Takeda Pharmaceutical, UCB Japan, outside the submitted work; and other authors declare no competing interests.

ACKNOWLEDGMENTS

We thank Naomi Tamura for the advice of statistical analysis. We appreciate BioRender.com for the creation of figures.

DATA AVAILABILITY STATEMENT

Data of fMRI are not publicly available and are stored locally, following national and Japanese laws on the protection of individuals with regard to the processing of personal data. Clinical data are available upon reasonable request. All data required to evaluate the conclusions are included in the article or uploaded as supplementary information.

REFERENCES

1. Logothetis NK. The underpinnings of the BOLD functional magnetic resonance imaging signal. J Neurosci 2003;23:3963-71.
2. Schrepf A, Kaplan CM, Ichesco E, Larkin T, Harte SE, Harris RE, et al. A multi-modal MRI study of the central response to inflammation in rheumatoid arthritis. Nat Commun 2018;9:2243.
3. Basu N, Kaplan CM, Ichesco E, Larkin T, Schrepf A, Murray AD, et al. Functional and structural magnetic resonance imaging correlates of fatigue in patients with rheumatoid arthritis. Rheumatology (Oxford) 2019;58:1822-30.
4. Basu N, Kaplan CM, Ichesco E, Larkin T, Harris RE, Murray A, et al. Neurobiologic Features of Fibromyalgia Are Also Present Among Rheumatoid Arthritis Patients. Arthritis Rheumatol 2018;70:1000-7.
5. Kaplan CM, Schrepf A, Ichesco E, Larkin T, Harte SE, Harris RE, et al. Association of Inflammation With Pronociceptive Brain Connections in Rheumatoid Arthritis Patients With Concomitant Fibromyalgia. Arthritis Rheumatol 2020;72:41-6.
6. Baliki MN, Petre B, Torbey S, Herrmann KM, Huang L, Schnitzer TJ, et al. Corticostriatal functional connectivity predicts transition to chronic back pain. Nat Neurosci 2012;15:1117-9.
7. Ichesco E, Peltier SJ, Mawla I, Harper DE, Pauer L, Harte SE, et al. Prediction of Differential Pharmacologic Response in Chronic Pain Using Functional Neuroimaging Biomarkers and a Support Vector Machine Algorithm: An Exploratory Study. Arthritis Rheumatol 2021;73:2127-37.
8. Abe N, Fujieda Y, Tha KK, Narita H, Aso K, Karino K, et al. Aberrant functional connectivity between anterior cingulate cortex and left insula in association with therapeutic response to biologics in inflammatory arthritis. Semin Arthritis Rheum 2022;55:151994.

9. Preti MG, Bolton TA, Van De Ville D. The dynamic functional connectome: State-of-the-art and perspectives. Neuroimage 2017;160:41-54.

10. Leonardi N, Van De Ville D. On spurious and real fluctuations of dynamic functional connectivity during rest. Neuroimage 2015;104:430-6.

11. Cottam WJ, Iwabuchi SJ, Drabek MM, Reckziegel D, Auer DP. Altered connectivity of the right anterior insula drives the pain connectome changes in chronic knee osteoarthritis. Pain 2018;159:929-38.

12. Cheng JC, Anzolin A, Berry M, Honari H, Paschali M, Lazaridou A, et al. Dynamic Functional Brain Connectivity Underlying Temporal Summation of Pain in Fibromyalgia. Arthritis Rheumatol 2022;74:700-10.

13. Aletaha D, Neogi T, Silman AJ, Funovits J, Felson DT, Bingham CO, 3rd, et al. 2010 rheumatoid arthritis classification criteria: an American College of Rheumatology/European League Against Rheumatism collaborative initiative. Ann Rheum Dis 2010;69:1580-8.

14. Rudwaleit M, Landewé R, van der Heijde D, Listing J, Brandt J, Braun J, et al. The development of Assessment of SpondyloArthritis international Society classification criteria for axial spondyloarthritis (part I): classification of paper patients by expert opinion including uncertainty appraisal. Ann Rheum Dis 2009;68:770-6.

15. Rudwaleit M, van der Heijde D, Landewé R, Akkoc N, Brandt J, Chou CT, et al. The Assessment of SpondyloArthritis International Society classification criteria for peripheral spondyloarthritis and for spondyloarthritis in general. Ann Rheum Dis 2011;70:25-31.

16. Smolen JS, Breedveld FC, Schiff MH, Kalden JR, Emery P, Eberl G, et al. A simplified disease activity index for rheumatoid arthritis for use in clinical practice. Rheumatology (Oxford) 2003;42:244-57.

17. Lukas C, Landewé R, Sieper J, Dougados M, Davis J, Braun J, et al. Development of an ASAS-endorsed disease activity score (ASDAS) in patients with ankylosing spondylitis. Ann Rheum Dis 2009;68:18-24.

18. Felson DT, Anderson JJ, Boers M, Bombardier C, Chernoff M, Fried B, et al. The American College of Rheumatology preliminary core set of disease activity measures for rheumatoid arthritis clinical trials. The Committee on Outcome Measures in Rheumatoid Arthritis Clinical Trials. Arthritis Rheum 1993;36:729-40.

19. Anderson JJ, Baron G, van der Heijde D, Felson DT, Dougados M. Ankylosing spondylitis assessment group preliminary definition of short-term improvement in ankylosing spondylitis. Arthritis Rheum 2001;44:1876-86.

20. Faillenot I, Heckemann RA, Frot M, Hammers A. Macroanatomy and 3D probabilistic atlas of the human insula. Neuroimage 2017;150:88-98.

21. Demertzi A, Tagliazucchi E, Dehaene S, Deco G, Barttfeld P, Raimondo F, et al. Human consciousness is supported by dynamic complex patterns of brain signal coordination. Sci Adv 2019;5:eaat7603.

22. Xia M, Wang J, He Y. BrainNet Viewer: a network visualization tool for human brain connectomics. PLoS One 2013;8:e68910.

23. Ohara PT, Vit JP, Jasmin L. Cortical modulation of pain. Cell Mol Life Sci 2005;62:44-52.

24. Letzen JE, Robinson ME. Negative mood influences default mode network functional connectivity in patients with chronic low back pain: implications for functional neuroimaging biomarkers. Pain 2017;158:48-57.

25. Yuan Y, Zhang L, Li L, Huang G, Anter A, Liang Z, et al. Distinct dynamic functional connectivity patterns of pain and touch thresholds: A resting-state fMRI study. Behav Brain Res 2019;375:112142.

26. Hess A, Axmann R, Rech J, Finzel S, Heindl C, Kreitz S, et al. Blockade of TNF-α rapidly inhibits pain responses in the central nervous system. Proc Natl Acad Sci U S A 2011;108:3731-6.

27. Rech J, Hess A, Finzel S, Kreitz S, Sergeeva M, Englbrecht M, et al. Association of brain functional magnetic resonance activity with response to tumor necrosis factor inhibition in rheumatoid arthritis. Arthritis Rheum 2013;65:325-33.

28. Hess A, Roesch J, Saake M, Sergeeva M, Hirschmann S, Neumann H, et al. Functional Brain Imaging Reveals Rapid Blockade of Abdominal Pain Response Upon Anti-TNF Therapy in Crohn's Disease. Gastroenterology 2015;149:864-6.

29. Schaible HG. Nociceptive neurons detect cytokines in arthritis. Arthritis Res Ther 2014;16:470.

30. May A. Chronic pain may change the structure of the brain. Pain 2008;137:7-15.

FIGURE LEGENDS

Figure 1. Distinct cluster patterns of dynamic functional connectivity in patients with inflammatory arthritis (IA).

(A) Schema of dynamic functional connectivity analysis. (**B)** Four patterns by cluster analysis of dynamic functional connectivity matrices in the retrospective dataset with absolute connection value > 0.2 rendered on brain view. (**C**) Statistically significant functional connections colour-weighted by ANCOVA-F statics comparing the cluster patterns.

Figure 2. The occurrence probability of dynamic functional connectivity patterns related to therapeutic responsiveness in IA patients.

(**A**, **B)** The likelihood of each coordination pattern occurrence associated with the patterns' probability distribution in (**A**) the first dataset and (**B**) the second dataset. *$P_{FWE} < 0.05$, **$P_{FWE} < 0.01$, ****$P_{FWE} < 0.0001$, ANCOVA adjusting age and sex with post-hoc Tukey-Kramer test. (**C**, **D)** Comparison of occurrence probability of each pattern according to therapeutic effectiveness in (**C**) the first dataset and (**D**) the second dataset. *$P < 0.05$, ANCOVA adjusting age and sex. Data are mean ± s.e.m. (**E, F)** ROC analysis for therapeutic effectiveness using the occurrence probability of cluster pattern 3 in (**E**) the first and (**F**) second dataset. (**G**, **H)** Pearson's correlation analysis between the occurrence probability of cluster pattern 3 and clinical parameters: **(G)** disease activity and **(H)** patients' global assessment in the consolidated dataset.

Figure 3. Therapeutic effectiveness in IA distinguished by dynamic functional corticocortical connectivity.

(A) Statistically significant functional connectivity with high functional corticocortical correlations in cluster pattern 3 compared with other cluster patterns color-coded by F statics calculated from ANCOVA adjusting age and sex with Tukey-Kramer test. (**B**, **C)** Transitions of averaged functional connectivity values between left anterior long IG and ACC with sliding windows as time series in IA patients with therapeutic effectiveness (red) and ineffectiveness

(blue) using (**B**) the first dataset and **(C)** the second dataset. Mixed model for a repeated measures design with AR(1) covariance structure adjusting age, sex and windows, was used. Data are mean (solid) ± s.e.m. (band).

Figure 4. The occurrence probability of corticocortical connectivity patterns

(**A**, **B)** Occurrence probabilities of corticocortical cluster pattern 3 in IA patients treated with (**A**) TNF-α inhibitors (n = 21) or (**B**) non-TNF-α inhibitors (n = 43) in the consolidated dataset. *P < 0.05, ANCOVA adjusting age and sex. Data are mean ± s.e.m. (**C)** Occurrence probabilities of corticocortical cluster pattern 3 before and after initiation of biologics. fMRI data of the second dataset were used. *P < 0.05, paired t-test. Data are mean ± s.e.m.

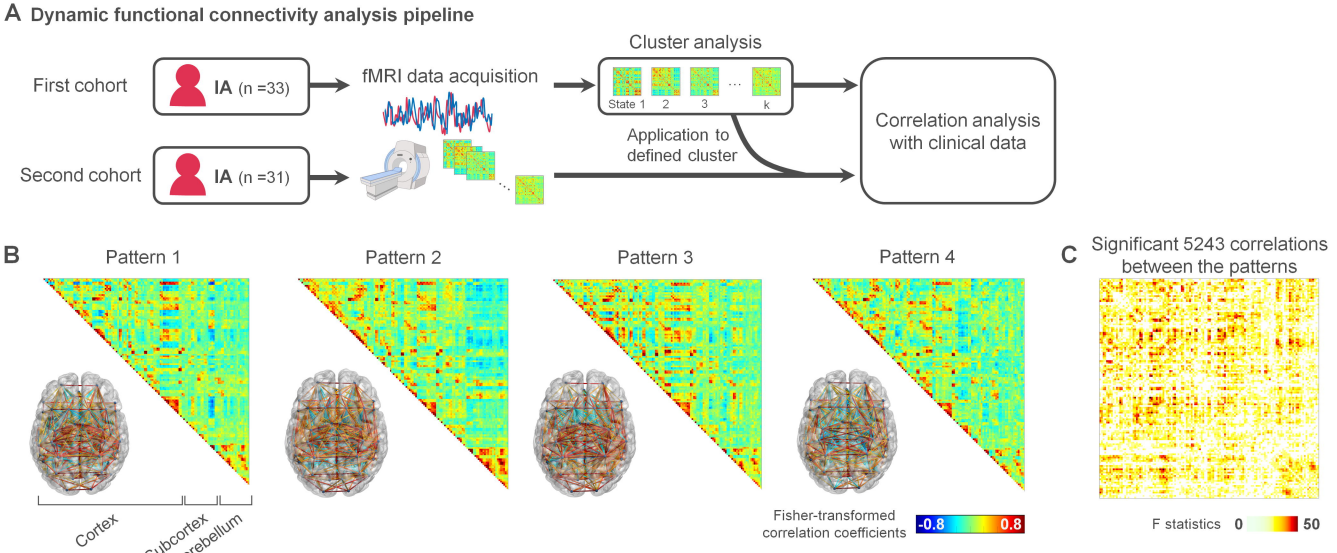
A Dynamic functional connectivity analysis pipeline
First cohort
IA (n =33)
Second cohort
IA (n =31)
fMRI data acquisition
Cluster analysis
State 1
2
3
k
Application to defined cluster
Correlation analysis with clinical data
B
Pattern 1
Pattern 2
Pattern 3
Pattern 4
Cortex
Subcortex
Cerebellum
Fisher-transformed correlation coefficients
-0.8
0.8
C
Significant 5243 correlations between the patterns
F statistics
0
50

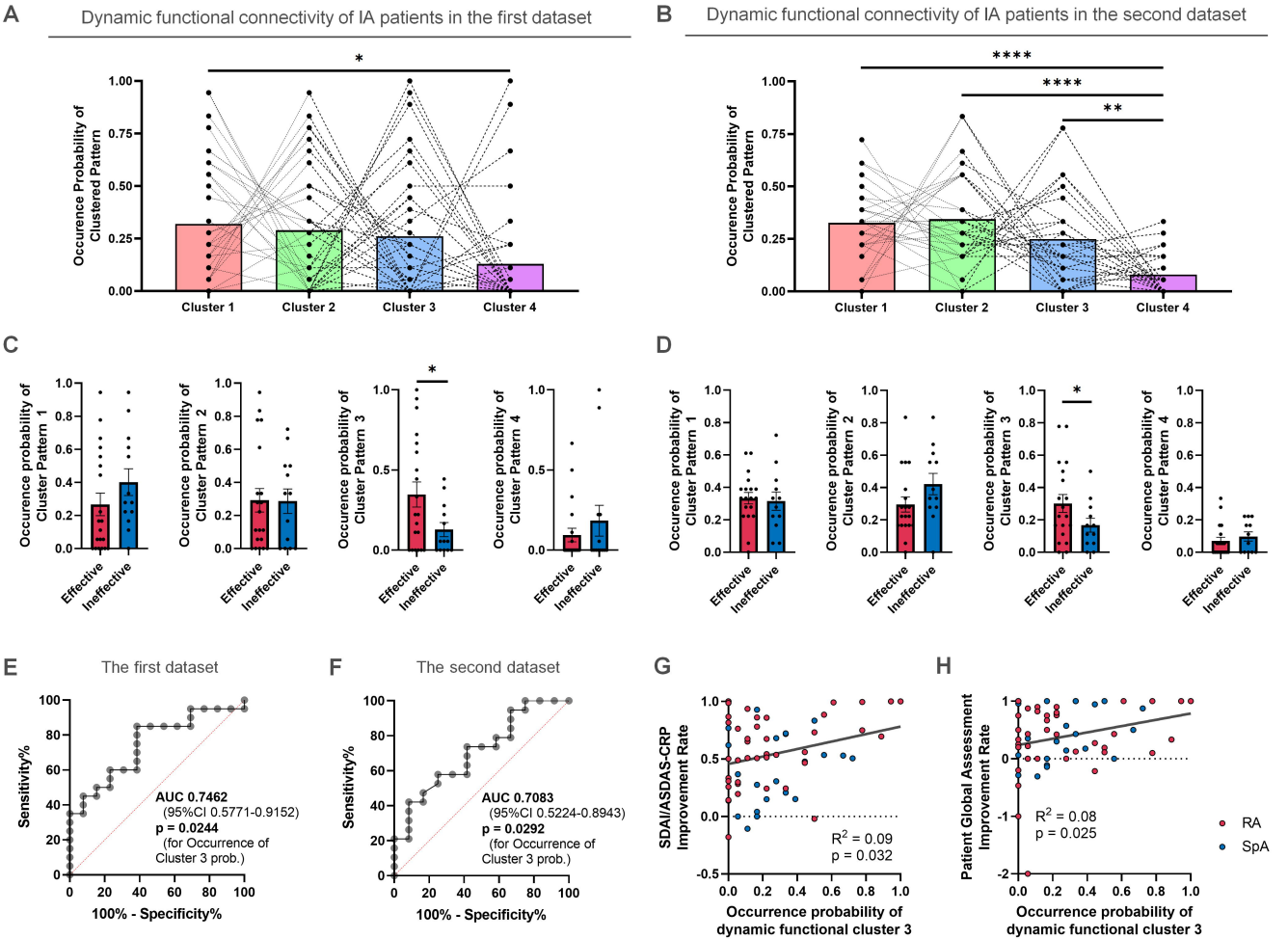
A
Dynamic functional connectivity of IA patients in the first dataset
Occurence Probability of Clustered Pattern
Cluster 1
Cluster 2
Cluster 3
Cluster 4
B
Dynamic functional connectivity of IA patients in the second dataset
C
Occurence probability of Cluster Pattern 1
Occurence probability of Cluster Pattern 2
Occurence probability of Cluster Pattern 3
Occurence probability of Cluster Pattern 4
Effective
Ineffective
D
E
The first dataset
Sensitivity%
100% - Specificity%
AUC 0.7462
(95%CI 0.5771-0.9152)
p = 0.0244
(for Occurrence of Cluster 3 prob.)
F
The second dataset
AUC 0.7083
(95%CI 0.5224-0.8943)
p = 0.0292
(for Occurrence of Cluster 3 prob.)
G
SDAI/ASDAS-CRP Improvement Rate
R2 = 0.09
p = 0.032
Occurrence probability of dynamic functional cluster 3
H
Patient Global Assessment Improvement Rate
R2 = 0.08
p = 0.025
RA
SpA

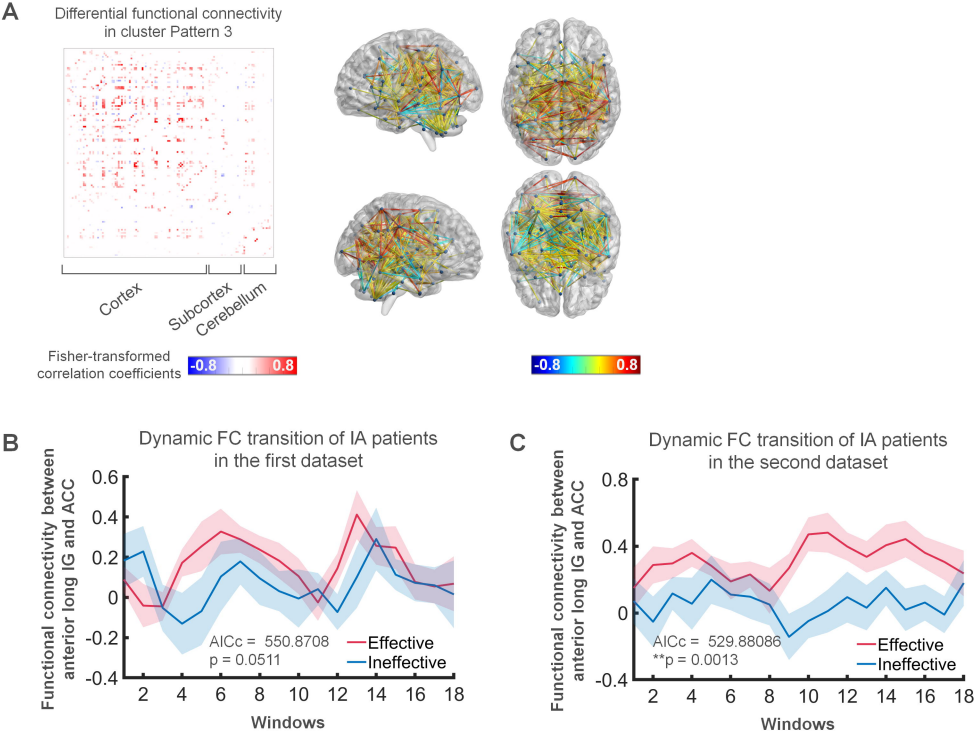
A
Differential functional connectivity
in cluster Pattern 3
Cortex
Subcortex
Cerebellum
Fisher-transformed
correlation coefficients
-0.8
0.8
-0.8
0.8
B
Dynamic FC transition of IA patients
in the first dataset
Functional connectivity between
anterior long IG and ACC
0.6
0.4
0.2
0
-0.2
-0.4
AICc = 550.8708
p = 0.0511
Effective
Ineffective
2
4
6
8
10
12
14
16
18
Windows
C
Dynamic FC transition of IA patients
in the second dataset
Functional connectivity between
anterior long IG and ACC
0.8
0.4
0
-0.4
AICc = 529.88086
**p = 0.0013
Effective
Ineffective
2
4
6
8
10
12
14
16
18
Windows

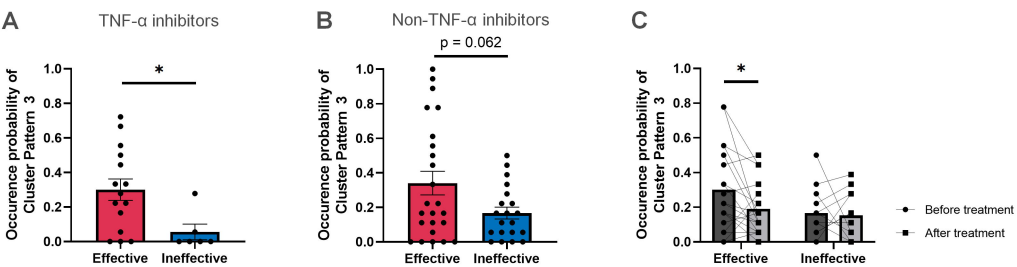
A
TNF-α inhibitors
*
Occurence probability of Cluster Pattern 3
1.0
0.8
0.6
0.4
0.2
0.0
Effective
Ineffective
B
Non-TNF-α inhibitors
p = 0.062
Occurence probability of Cluster Pattern 3
1.0
0.8
0.6
0.4
0.2
0.0
Effective
Ineffective
C
*
Occurence probability of Cluster Pattern 3
1.0
0.8
0.6
0.4
0.2
0.0
Effective
Ineffective
Before treatment
After treatment